JOURNAL OF OPTOELECTRONICS AND ADVANCED MATERIALS Vol. 12, No. 7, July 2010, p. 1556 - 1561

Effect of surface rubbing on polarization behavior and electro-optical properties of holographic polymer-dispersed liquid crystals (*HPDLCs*)

M. BEHZADI RAD, N. HOSAIN NATAJ, E. MOHAJERANI*, H. NEMATI
Laser and Plasma Research Institute (LAPRI) of Shahid Beheshti University, G.C., Evin, Tehran, Iran

Effect of surface rubbing on the polarization and electro-optical properties of holographic polymer dispersed liquid crystals (*HPDLCs)* was studied in details to approach to the optimal situation in different applications. The polarization-dependence of the diffracted intensities of *s*-and *p*-polarized probe beam and polarization rotation of samples were investigated. It is shown that TN sample can rotate polarization of the diffracted probe beam, rotated by 10°-20°, depending on the incident polarization. Electro-optical investigation shows that the *NA* and *TN* samples have the fastest and slowest response time in switch-on state and, inversely, slowest and fastest response time in switch-off state, respectively.

(Received March 16, 2010; accepted July 14, 2010)

Keywords: Liquid crystal, Holographic gratings, Surface rubbing, Polarization-dependence

1. Introduction

Holographic polymer dispersed liquid crystals (*HPDLCs*), have recently attracted more attention for their use in the great number of the optical components such as reflecting flat-panel displays[1,2], optical interconnectors[3], diffraction lenses with switchable focus [4,5], optical data storage [6], and image capture applications [7]. *HPDLC* devices may be considered as periodic layers of *LC* rich droplet planes and cured photosensitive polymer planes. The periodic structure is produced by photo- polymerization induced phase separation (*PIPS*) process under the influence of two interfering laser beams [8,9]. The composite is made of a homogeneous photosensitive pre-polymer mixture and a liquid crystal molecule. In the bright regions of the interference pattern, the polymerization occurs more rapidly and the *LC* molecules diffuse to dark regions while the monomers diffuse to the bright regions [10]. As a result, the *LC* droplets and polymer layers are distinctly formed in the dark and bright regions, respectively; and due to the phase separation, an optical grating is formed. The difference between refractive index of *LC* and polymer planes results in the diffraction of the incident light in absence of external electric field. When an external electric field is applied (on-state), *LC* molecules in the droplets align in the direction of the applied electric field so that the refractive index changes to the ordinary refractive index of the liquid crystal, n_o. If ordinary refractive index of the liquid crystal, n_o, is close to the refractive index of the polymer, n_p, the grating vanishes and the sample becomes transparent. Cells with no alignment (*NA*), twisted nematic (*TN*) or homogeneous cells (*HG*) might be used to fabricate such devices. The surfaces in the *NA* cells have no alignment; so they do not induce any particular orientation to *LC* molecules, while, in the *TN* and *HG* cells, there are perpendicular and parallel rubbing alignments on the surfaces, respectively, which induce specific orientation to *LC* molecules, according to the rubbing direction.

Recently many research groups have tried to optimize and evaluate new materials, exposure times, polarization effect, temperature effect and preparation procedures [2,3,5], to achieve better reflection or diffraction efficiencies, lower switching voltages, and shorter response times.

In this article effect of surface rubbing on the Electro-Optical and polarization behavior of holographic gratings are studied and by comparing results between different samples, optimal rubbing in different applications are created.

2. Experimental

2.1 Materials and samples preparation

The materials used to fabricate the pre-polymer mixture were, trimethylolpropane triacrylate (*TMPTA*), as monomer, *N*-vinylpyrrollidone (*NVP*), as crosslinking monomer, rose bengal (*RB*) as photoinitiator, *N*-phenylglycine (*NPG)*, as coinitiator, and S-271 POE sorbitan monooleate as surfactant, all from Aldrich. The ratio of TMPTA/NVP/S-271/NPG/RB was 62/25/10/2/1 by weight for all samples. The refractive index of the cured polymer was 1.522 at 632.8 nm [11]. After mixing pre-polymer composites, the liquid crystal E7 from Merck with the ordinary refractive index of no=1.521, and birefringence of Δn=0.225 was increased to the mixture. The pre-polymer and *LC* were mechanically blended at

65/35 weight ratio, correspondingly, at 30 °C in all samples. Readymade *NA*, *TN* and *HG* cells formed by two *ITO* coated glass plates separated by *d*=8 µm thick spacer, were filled with the photosensitive pre-polymer/*LC* syrup by means of the capillary flow.

2.2 Experimental set up

As shown in Fig .1, the samples are placed within the intersection of two laser beams from a 532 nm second harmonic *Nd:YAG* laser, which were in the *p*-polarized state(*p*-polarized, the polarization direction parallel to the grating vector of the laser induced grating). The laser beam was first expanded and collimated to achieve 4 mm diameter beams over the *LC* cell. The power of each pump beams was 19 mW and the exposure time was 5 min for all samples. After exposing the samples under intersecting laser beams, the samples were further cured for 15 min by mercury lamp.

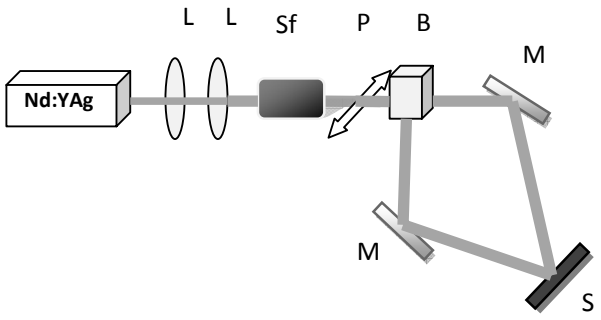

Fig. 1. Experimental set-up used to record diffraction gratings (L: collimator lens, Sf: spatial filter, P: polarizer, B: beam splitter, M: mirror, S: sample).

After photocuring, samples were mounted on a rotation stage with rotation axis orthogonal to the grating vector to measure the diffracted intensity. A non-polar He-Ne laser with 632.8 nm wavelength and beam diameter of approximately 3 mm was used to probe the samples at the exact Bragg angle, as shown in the Fig. 2. The power of the incident *He-Ne* probe beam was ~1 mW, which is low enough to prevent optical field induced reorientation of nematic molecules [12]. The polarization of the incident light was controlled by a linear polarizer between *p*-polarization and *s*-polarization to investigate the dependency of diffracted intensity on the incident polarization. In order to study the rotation of probe beam polarization, second linear polarizer was placed between detector and samples.

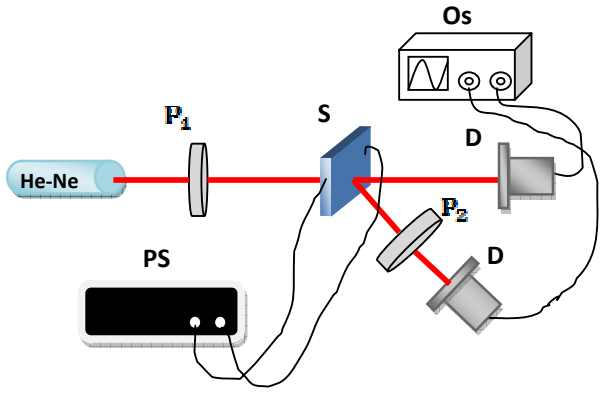

Fig. 2. Experimental set-up used to probe HPDLC samples (P: polarizer, S: sample, D: detector, Os: oscilloscope, PS: ac power supply).

The electro-optical properties were checked by applying alternating square voltage at a sufficiently high frequency of 1 kHz, to avoid unwanted dc screening and current effects. Two photodiode detectors were placed ~30 cm behind the sample to detect both diffracted and transmitted beams. An oscilloscope was used to monitor output of the detectors. Data in the each step were successively measured for all samples at the same condition.

3. Results and discussions

In order to compare samples prepared by *NA*, *TN* and *HG* cells, the effect of the probe beam polarization state, polarization rotation in the samples and electro-optical properties of different samples are studied.

3.1 Studying the probe beam polarization state

In order to study the effect of the incident light polarization state on the diffracted intensity, probe polarization was changed from 0˚ to 180˚. Figure.3 shows the diffracted intensity versus polarization degree of the probe beam for all three samples. Maximum intensities are achieved when the polarization of incident light is parallel to the pump polarization state (*p*-polarized). Furthermore, the *HG* sample shows largest diffracted intensity in comparison with the other samples, while the *TN* shows the least intensity. It could be inferred from subsidence of curves in Fig.3, that homogeneous and *TN* cells show the most and least diffracted intensity-dependency on the polarization of the probe beam, respectively.

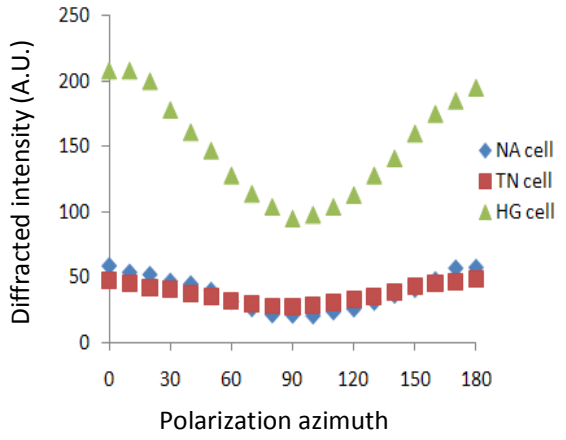

Fig. 3. Effect of the light polarization on diffracted intensity.

These maximum diffracted intensity and difference in subsidence of curves, can be justified by considering the optical electric field and surface rubbing effect. It is shown that these phenomena are effective on the anisotropy of holographic gratings.

During the photocuring process, the optical field (**E**) of polarized light induces an electrical instantaneous dipole (P) in *LC* molecules [13,14], that it can rotate molecule directors along
the optical electric filed direction [15], as given in equation (1).

$$\tau = E \times P \tag{1}$$

Indeed, this induced electrical torque affects on the orientational order of nematic *LC* molecules. Therefore, during polymerization the *LC* molecules tend to orient to a new configuration parallel to the direction of the polarization of light (*p*-polarized). The total free energy of the system in the presence of an optical field and the optical dipolar interaction energy (F_{op}) can be expressed as [14]

$$F_{op} = -\frac{\varepsilon_\perp}{4\pi}E^2 - \Delta\varepsilon\frac{(\mathbf{n}\cdot\mathbf{E})^2}{4\pi} \tag{2}$$

(Where **n** indicates unit vector parallel to the long molecular axis, $\varepsilon_\perp$ and $\Delta\varepsilon$ are perpendicular dielectric permittivity and dielectric anisotropy, respectively). It confirms our expression that the system reaches the minimum free energy when the $\vec{n}$ vector is parallel to the optical electric field. Due to this orientation of molecules, a linear polarized light with the same polarization as the pump beams experiences maximum refractive index mismatch between *LC* droplet (extraordinary refractive index) and polymer regions.

In addition, the alignments in the cell surfaces induces an orientation parallel to the rubbing direction to the *LC* molecules [16] which are in the nearest droplets to the surfaces. Based on the original fabrication, this alignment in the *HG* cell is along the pump polarization direction (*p* polarization) and therefore the polarization field and rubbing direction intensify the effect of each other, and then more molecules in the droplets orient toward the induced direction. This leads the *HG* sample to have the highest diffracted intensity for *p*-polarized incident light and also have highest subsidence among all the curves because of the more molecules orientation along the induced direction. It means that the *HG* sample shows a high diffracted intensity-dependency on the polarization of light. In contrast, in the 90°-*TN* cell, one of the surfaces has the inverse surface rubbing (*ISR*) effect which is against the effect of the optical field and the rubbing of the other surface. The *ISR* effect can reduce effect of optical field on the *LC* orientation. In the *TN* sample, light sees the refractive index matching in region near to the surface with *ISR* effect (surface with perpendicular alignments to the *p*-polarized direction). In the case of *NA* cell, the surfaces are without alignment and then, induced direction by polarization field is the only force which affects on the *LC* molecules orientation. Since the probe light sees the extraordinary refractive index of *LC* molecules in the parallel orientation to the pump polarization field and because it is thoroughly mismatch with refractive index of polymer planes, it is cleared that diffracted intensity of the *HG* sample should be higher than the other samples due to the intensification of effects. Since the *NA* sample curve placed between *TN* and *HG* curves, it can be understood that surface rubbing has stronger effect than the polarization field to orientation of *LC* molecules in our samples. By considering strong *ISR* effect in *TN* sample and intensification of the induced direction in the *HG* sample, intermediate behavior of the *NA* sample is justifiable.

3.2 Polarization rotation

Nematic *LC*s show strong optical anisotropy and the resultant diffractive devices with nematic *LC*s are expected to enable the control of both the propagation and the polarization states of the light beam. In a condition which a TN cell was filled with only nematic *LC* and also gratings fabricated with alternative TN and homogeneous layers, device acts as polarization rotator with polarization plane rotating in alignment with molecular layer twist [17,18]. Effect of the samples on the polarization of incident light was found with fixing polarization state (in *s*-and *p*-polarization) by a linear polarizer in front of the sample and changing the polarization angles with another adjustable linear polarizer, which placed behind the sample. Fig. 4 illustrates polarization rotation effect of the three samples on the incident light in the *s*-and *p*-polarized states of the first polarizer, distinctly, in form of diffracted intensity as a function of polarization angle. As seen, *TN* sample has 20° rotation in *p*-polarized and 10° rotation for *s*-polarized state in diffracted light.

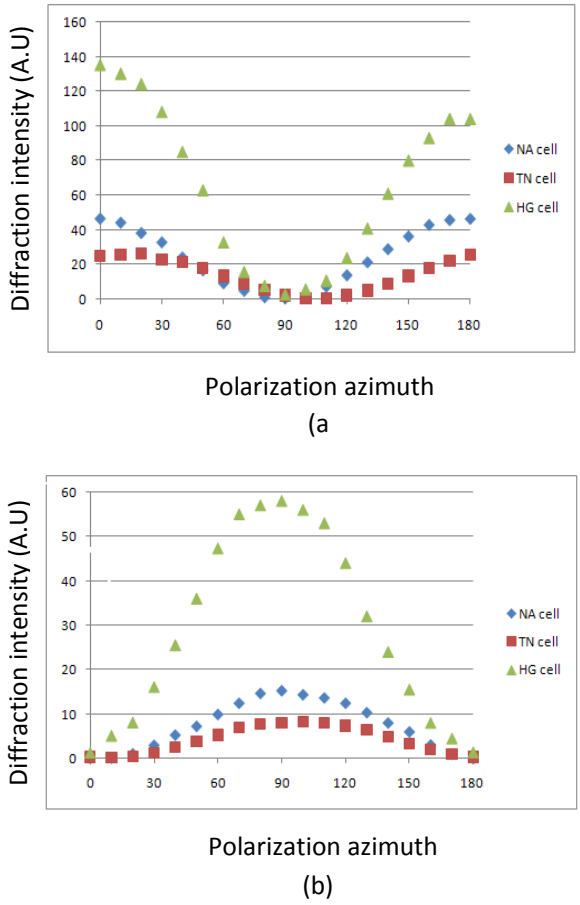

Fig. 4. Polarization rotation in (a) p–polarized and (b) s-polarized incident light for three samples. The used arbitrary unit for diffracted intensity in curves is same and comparable.

It is while the *HG* and NA samples don't show sensible rotation effect on the polarization of light. It means, only *TN* sample acts as a partially polarization rotator device for polarized incident light. Polarization rotation in *LC* devices can be expressed as Jones matrixes [15-17]. With considering polarization state of the incident and diffracted light, the polarization rotator Jones matrixes for *TN* sample can be written as

$$R_p(\theta) = \begin{bmatrix} \cos(2\theta)^\circ & \sin(2\theta)^\circ \\ -\sin(2\theta)^\circ & \cos(2\theta)^\circ \end{bmatrix}$$
$$R_s(\theta) = \begin{bmatrix} \cos(1\theta)^\circ & \sin(1\theta)^\circ \\ -\sin(1\theta)^\circ & \cos(1\theta)^\circ \end{bmatrix} \quad (3)$$

Which satisfy the vector Jones equation of

$$J_{diff} = R(\theta) \cdot J_{inc} \quad (4)$$

Where $R_p(\theta)$ and $R_s(\theta)$ are polarization rotator matrixes for *s*-and *p*-polarized state of incident light and J_{diff} and J_{inc} are diffracted and incident light Jones matrices, correspondingly.

This effect and the insignificant effect of *HG* and *NA* samples are referred to nature of the molecular orientation in the cells due to the rubbing direction effect. The rotation of polarization in our *TN* sample is less than reported results for *LC* gratings [17].

This difference is because of the *HPDLC* gratings have formed by alternative polymer and *LC* layers and since *LC* layers consist of the distinct droplets which don't influence to each other. So the twisting effect is limited to the droplets near to the surfaces, while the central droplets have independent orientation, see Fig. 5. Therefore, polarization rotation effect in the holographic *TN* grating sample decreases in comparison with *LC* gratings. However, it can be significant effect for different applications

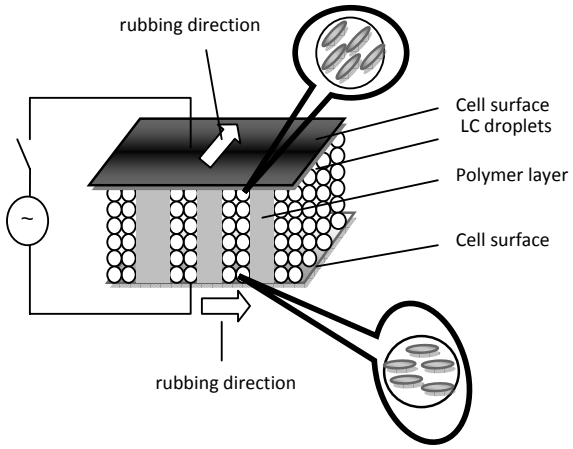

Fig. 5. Schematic of the orientation of LC molecules in the droplets near the two rubbed surfaces in TN sample.

3.3 Electro-optical switching

For switching operation of *HPDLC*s, it is of greatest interest to understand the dependence of the diffracted intensity on the external electric field. The electro-optical switching behavior was investigated for all the samples in the same condition. Fig. 6 plots diffracted intensity as a function of driving electric field for the three samples. As seen, in all samples the diffracted intensity decreases with increasing the external voltage. This decreasing in the diffracted intensity shows that in the case of *NA* sample, plot subsides with a steeper slope and tends to be zero quickly. While two other samples after 25 V_{rms}/μm take a smooth slope and decrease to zero gradually. The conductivity of the samples was originally so high that the voltage could not be increased further before they were completely switched. However, it can be understood from variation of the slopes that *NA* sample will be switched in lower external electric field. Thus, driving voltage for *NA* sample, which is an important parameter for gratings, is lower than *TN* and *HG* samples. The threshold electric

field was also measured for samples that were the same for all in ~2.12 V_{rms}/µm.

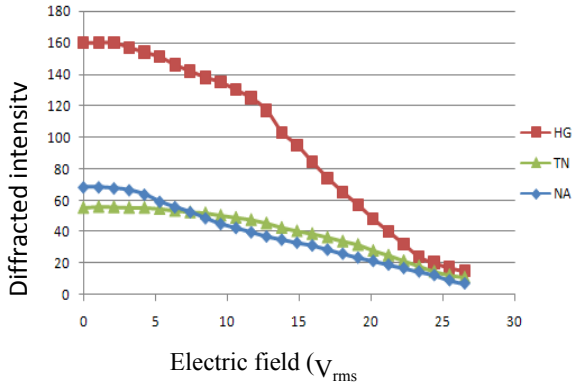

Fig. 6. Diffracted intensity as a function of applied electric filed.

The Surface rubbing increases the anchoring energy of the *LC* droplets in the *LC*/polymer composites and as a result the required electric field for reorientation of *LC* molecules increases [19]. When an external electric field is applied, first, the molecules in the central droplets start to align toward the electric field direction [19] in all the samples that cause the samples have almost the same threshold electric field value. After that, with increasing the voltage, the molecules in the droplets, which are closer to the surfaces and consequently are more impressible from surface rubbing, begin to reorient along the electric field direction. The anchoring energy In the *TN* and *HG* cells, due to the surface rubbing effect is higher than *NA* sample. Therefore, the required electric field to overcome the anchoring energy and to switch the *TN* and *HG* samples is higher than the *NA* sample. This high switching electric field causes slope of the curves to be smooth and reach zero, gradually.

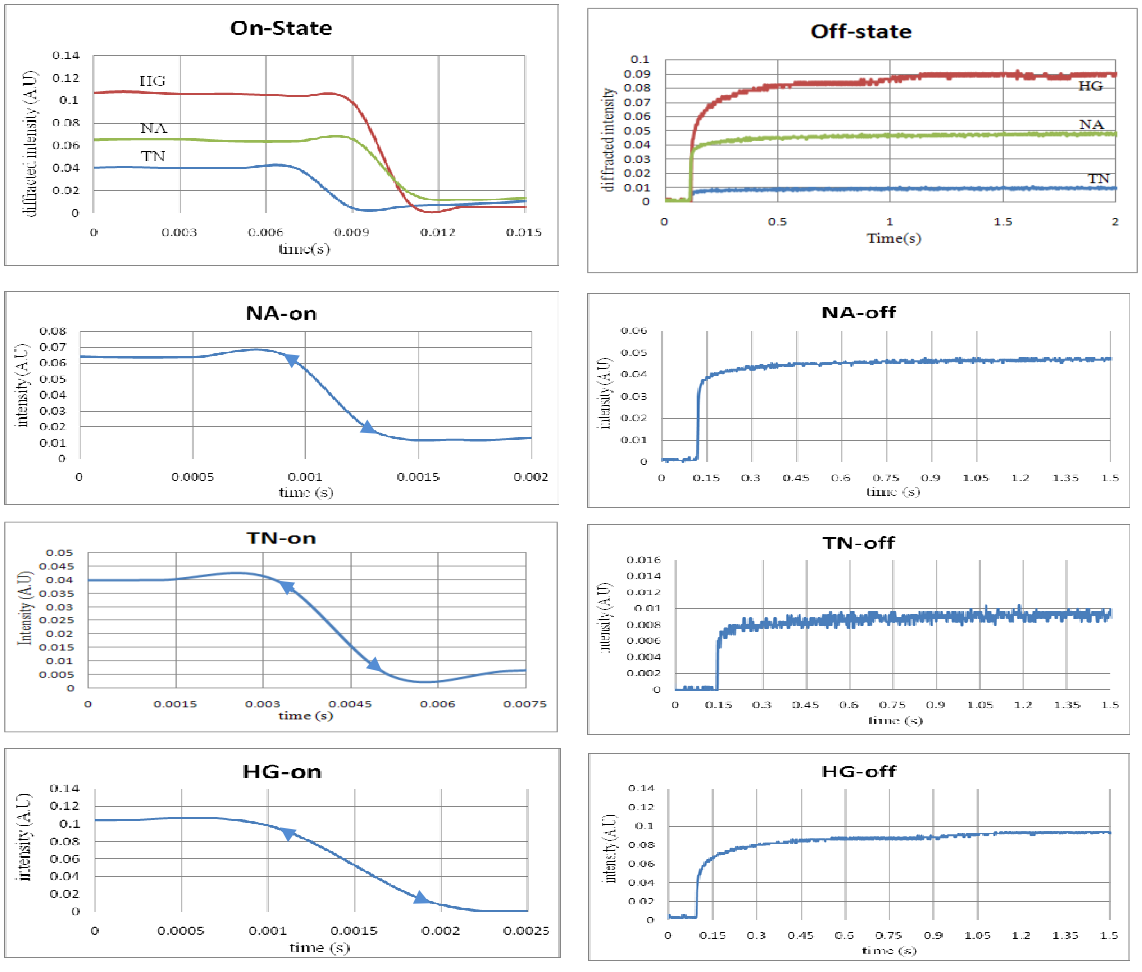

(a) (b)

Fig. 7. Response time of three samples in (a) on-state and (b) off-state.

Response time is a very important parameter for almost every *LC* device. We measured the holography gratings response time by using a square voltage at f =1 kHz between 0 and ~26.5Vrms/μm electric field. Figure.7 shows the response time of the samples in switch-on and switch-off states in form of diffracted intensity as a function of time. The samples have rise time (90% to 10% diffracted light intensity change in the switch-on state) in the range of submillisecond, except for *TN* sample and decay time (10% to 90% diffracted light intensity change in the switch-off state) in the range of millisecond, which were presented in Table 1. Response time is defined as the summation of rise and decay times [20]. It can be extracted from Table 1 that *NA* sample has the fastest rise time and the slowest decay time. In the *NA* cell molecules experience weaker anchoring energy from the surfaces, therefore, in turning on the voltage, molecules orient along the external electric field quickly. Alternatively, it is known that *LC* domains which require stronger fields for reorientation should possess faster decay time than domains that reorient under the weaker fields [21,22]. Then in the *HG* and *TN* samples which have a high anchoring energy, the molecules tend to reorient quickly to their initially relaxation states which have been determined by surface rubbing as seen in the fig.7 and Table 1. The TN sample, because of disorder in the orientation of molecules which are due to the inducer forces (ISR and surface rubbing effects), has slowest and fastest rise and decay time, respectively.

Table 1. Rise and decay response time of samples to applied electric field.

sample	Rise time(μs)	Decay time(ms)
NA	~ 377	~ 515
HG	~ 924	~ 461
TN	~ 1586	~ 364

4. Conclusions

In summary, we investigated the effect of surface rubbing on the polarization properties of anisotropic *HPDLC*s, which were fabricated in three different cells. The experimental results showed that the samples are polarization sensitive. It was observed that for all the samples, the maximum diffracted intensities are achieved when the polarization of the incident light is parallel and similar to the pump polarization and also it was demonstrated that the *HG* sample shows the greatest diffracted intensity-dependency on the polarization of the probe light.

The highest and the lowest diffracted intensities were observed in the *HG* and *TN* samples, respectively. Investigation of the polarization rotation effect demonstrated that only the *TN* sample can rotate incident light polarization by 10°-20°, depending on the incident polarization. Moreover, electro-optical studies showed that the sample without surface rubbing (*NA*) is switched in the lower external electric field with the fastest rise time and slowest decay time, while the *TN* sample shows slowest rise time and fastest time to be relaxed in switching-off state (decay time).

Acknowledgements

Authors would like to thank Shahid Beheshti University, G.C. for their supports.

References

[1] C. C. Bowley, et al. Appl. Phys. Lett**. 76**, 523 (2000).
[2] K. Kato, et al, Jpn. J. Appl. Phys., Part 1. **38**, 1466 (1999).
[3] L. V. Natarajan , et al, Proc. SPIE **3148**, 182 (1997).
[4] L. H. Domash, et al. Proc. SPIE. **188**, 2689 (1996).
[5] M. Popovich, S. Sagan, SID Digest of Technical Papers. **31**, 1060 (2000).
[6] F.Simoni, et al, Chem. Phys. **245,** 429 (1999).
[7] T. G.Fiske, et al SID Digest of Technical Papers **31,** 1134 (2000).
[8] K. Tanaka, et al, J. of the SID **2,** 37 (1994).
[9] H. Kogelnik, The Bell System Technical J. **48,** 2909 (1966).
[10] C. C. Bowley, G. P. Crawford. Appl. Phys. Lett**. 76,** 2235 (2000).
[11] Y. J. Liu, et al Appl. Phys. Lett**. 86**, 041115 (2005).
[12] M. Jazbinsek, et al,J. Appl. Phys**. 90,** 3831 (2001).
[13] I. C. Khoo, W. E. Leonhard, J.physrep. **471,** 221 (2009).
[14] F. W. Deeg, M. D. Fayer, J.Chem. Phys. **91,** 2269 (1989).
[15] H.Ono, et al, Jpn.J.Appl.Phys.**44,** 306 (2005).
[16] F. Du, et al, Optics express. **11**, 2891 (2003).
[17] B. A. Saleh, M.C. Teich, Fundamentals of photonics, (John Wiley & Sons, New York, 1991).
[18] T. Sasaki, et al, Jpn J. Appl. Phys. **46,** 698 (2007).
[19] P. S. Drzaic, Liq. Crys. **33,** 1286 (2006).
[20] B. K. Kim, S. H. Kim, J. Polym. Sci., B: Polym. Phys. **36,** 55 (1998).
[21] Y. K. Fung, et al, Proc. Eurodisplays. **93**, 157 (1993).
[22] K. Kato, et al, Jpn. J. Appl. Phys. **32**, 4594 (1993).

*Corresponding author: e-mohajerani@sbu.ac.ir